Three-photon cascade from single self-assembled InP quantum dots

J. Persson,[1,*] T. Aichele,[2] V. Zwiller,[2,†] L. Samuelson,[1] and O. Benson[2]
[1]*Solid State Physics/The Nanometer Consortium, Lund University, P.O. Box 118, 221 00 Lund, Sweden*
[2]*Nano-optics, Physics Department, Humboldt University, D-10117 Berlin, Germany*
(Received 7 November 2003; revised manuscript received 23 February 2004; published 25 June 2004)

We present photon correlation measurements performed on single self-assembled InP quantum dots in a GaInP barrier. Correlation measurements done under continuous excitation reveal a pronounced antibunching dip for the emission from the single exciton, the bi-exciton, and the tri-exciton. Cross-correlations between the different emission lines are used for line identification. We have correlated the photon emission from the exciton and the bi-exciton, as well as the emission from the bi-exciton and the tri-exciton. The asymmetric results of these cross-correlations clearly demonstrate a three-photon cascade as the tri-exciton recombines to the ground-state via the bi-exciton and the exciton. A rate-equation model was used to fit the measurements in support of the experimental conclusions.

DOI: 10.1103/PhysRevB.69.233314 PACS number(s): 78.67.Hc, 78.55.Cr, 73.21.La, 42.50.Dv

Optical investigations of individual quantum dots yield functionalities that are not accessible with ensembles of dots. Single photon sources have been realized in a number of different systems, such as single atoms, molecules, or color centers.[1–5] In particular, reliable sources of single photons are required for experiments in the fields of quantum cryptography and quantum computation.

Single semiconductor quantum dots are attractive nonclassical light sources as their properties can be engineered, they do not suffer from photobleaching, and can be integrated into complex semiconductor structures to make monolithic devices such as microcavities and pn-junctions. Single quantum dots have been shown to be good sources of nonclassical light, i.e., single-photon sources,[6–9] but also sequences of photons through the radiative cascade of bi-excitons into excitons.[10–12] In such a cascade, each photon in a pair has a unique wavelength, and cross-correlation measurements can identify the exciton from the bi-exciton. It has been speculated that nonclassical polarization correlations between photons may occur in such a cascade.[13] However, only classical polarization correlations have been observed so far.[14] Photon correlations between photons emitted from molecule pairs have also been measured to study coupling via resonant energy transfer.[15]

Early attempts using Stranski-Krastanow grown quantum dots to generate single photons were based on InAs quantum dots [7–9] emitting in the 870−950 nm range, but recent reports include single photon generation at visible wavelengths,[16–18] suitable for efficient detection using silicon based single photon detectors.

In this article, we present photon correlation measurements and use the results to understand the relation between the individual emission lines of a single quantum dot. We observe antibunching on the emission of the exciton, the bi-exciton, and the tri-exciton and we perform cross-correlation measurements on the cascading of tri-excitons into excitons via the bi-exciton state. This is a tool that enables identification of the precise nature of all the emission lines from a single quantum dot under weak excitation, and we demonstrate the potentials by identifying a tri-exciton line in a group of closely spaced lines.

We have used Stranski-Krastanow grown InP quantum dots embedded in a GaInP matrix. The sample was grown by metal-organic vapor-phase epitaxy at low pressure. Initially a lattice matched layer of $Ga_{0.51}In_{0.49}P$ was grown on GaAs. Subsequently, 1.9 monolayers of InP was grown, which formed quantum dots after a 12-s growth interrupt. A final cap layer of 100 nm GaInP was then grown.[20] Previously it has been shown that the dots grow in a bi-modal fashion and that the slightly n-type GaInP plays a major role in charging of the larger dots.[21] However, for small enough quantum dots, the dots used in this study, the confinement prevents the charging and the dot is neutral.[19]

By imaging the sample through a narrow bandpass filter, the density of dots emitting at around 680 nm was estimated to be about 10^8 cm^{-2}. In order to enable multiple measurements on the same dot and the use of different measurement setups, a gold film with 460-nm circular apertures[22] and a coordinate system was defined on the sample. A frequency doubled neodymium doped yttrium-orthovanadate ($Nd:YVO_4$) laser emitting at 532 nm was used as a continuous excitation source.

The sample was mounted in a cold finger cryostat and all measurements reported here were performed at 8 K. The emission was collected using a cover-glass-corrected objective with 0.75 numerical aperture, providing a spatial resolution of approximately 0.5 μm. The collected luminescence was spectrally filtered using bandpass filters [full-width at half maximum (FWHM) 0.5 and 1.0 nm] and spatially filtered with a pinhole. The signal was either sent to a charge-coupled device (CCD) camera for imaging, to a spectrometer, or to a Hanbury-Brown and Twiss interferometer for time-correlation measurements.

Single quantum dots were selected by imaging a dot through the pinhole, see Fig. 1. For spectroscopy, the emission was dispersed by a single 0.5-m spectrometer and the signal was detected with a liquid-nitrogen-cooled CCD camera. In order to vary the excitation power density we used neutral density filters. For the correlation measurements, avalanche photodiodes [APD's, (EG&G) single photon counting modules] were used and correlation events were collected

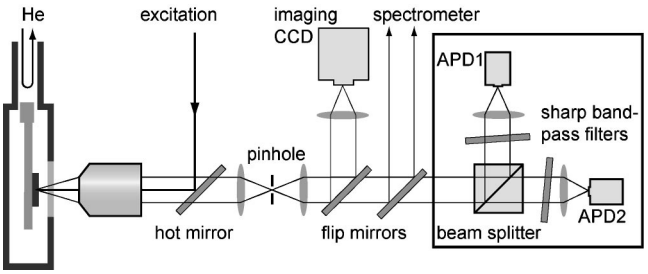

FIG. 1. The experimental setup used for the photon correlation measurements.

into 37-ps time bins using a PicoQuant TimeHarp 200 correlation card. The time resolution of the setup was determined by measuring the autocorrelations of the 150-fs pulses from a mode-locked Ti:Sapphire laser, and gave a time-resolution of 800 ps. A sketch of the experimental setup can be seen in Fig. 1.

Figure 2 shows the photoluminescence spectra of the quantum dot used in the experiments, taken under various excitation power densities. In all the figures, the reference excitation power density P_0 was kept constant at 0.1 W/cm^2. This is a typical spectral behavior, in terms of line spacing and power dependence, for an InP dot emitting in this energy range.[19] At low excitation power density, a single sharp emission line (at 1.8155 eV) is present in the spectrum (X_1). As the excitation power is increased, an additional line (X_2) appears about 1.5 meV below the exciton emission. As we increase the excitation power further, additional lines appear. The lines are as sharp as our setup can resolve with FWHM on the order of 100 μeV. The integrated photoluminescence

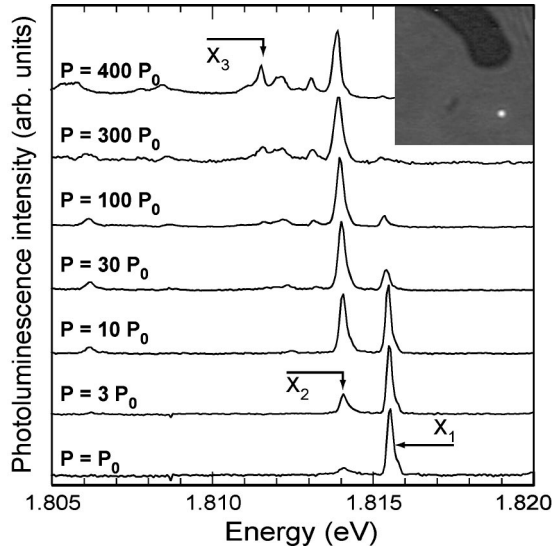

FIG. 2. Power dependent spectroscopy of a small single InP quantum dot showing the lines used in the correlation measurements, $P_0 = 0.1$ W/cm^2. Lines X_1 and X_2 have previously been attributed to the single exciton and the bi-exciton emission (Ref. 19). The inset is a 40 μm $\times$ 40 μm photoluminescence image of the sample recorded using a bandpass filter centered at 1.815 eV showing an aperture containing a single dot emitting at this energy and a part of the coordinate system defined on the sample.

intensity of X_1 increases linearly with the excitation power density whereas X_2 increases quadratically. The behavior is a good indication of excitonic and bi-excitonic emission, respectively. The lines appearing at high excitation power density, e.g. X_3, are attributed to a multiexciton of higher complexity. We will assume this line (X_3) to originate from a tri-exciton and we will provide experimental data to prove this.

For such a complex exciton, it is necessary to invoke additional states to the single-particle ground-states of the quantum dot. In this system, the conduction-band level-splitting is on the order of 50 meV,[19] and it should thus be possible to observe emission at an energy roughly 50 meV above the exciton emission line. However, at this energy there is strong competition with the wetting layer and the matrix material of the structure, hiding the interesting emission. It is nevertheless possible to study such states since the event of, e.g., a tri-exciton recombining and leaving the dot with an excited bi-exciton has an energy in the same range as the exciton and the bi-exciton.

In order to sort out the relation of the individual lines, we have performed photon correlation measurements. The simplified decay-chain of a tri-exciton (in principle the exciton is split in four levels and the excited bi-exciton in eight, due to spin interactions) is sketched in Fig. 3(a). Using the setup in Fig. 1, sending the spatially and spectrally filtered emission from a single dot and emission line to the Hanbury-Brown and Twiss interferometer, auto-correlation measurements were performed. Figures 3(b)–3(d) show the measured photon count distribution $n(\tau)$ for the exciton (X_1), the bi-exciton (X_2), and the tri-exciton (X_3), respectively, of the dot in Fig. 2. The normalized measured photon count distribution $n(\tau)$, is equivalent to the second-order correlation function $g^{(2)}(\tau)$ as long as the measured time separation τ between photon pairs is much smaller than the mean time between detection events.[23] We observe an almost perfect antibunching dip for the exciton and the bi-exciton, taking into account the response-time of our photodetectors.[18] The dashed lines in Figs. 3(b)–3(d) show the exponential fits of a perfect antibunching dip convoluted with the 800-ps response time of the correlation setup. The dip is significantly shallower for the tri-exciton. We explain this with the fact that at powers needed for the tri-exciton to appear, the tails of several emission lines are transmitted by the bandpass filter, degrading the antibunching dip.

Additional information can be gained by performing cross-correlation measurements between the individual emission lines. Figure 4(a) shows the cross-correlations of the exciton and the bi-exciton of the same dot under different excitation power densities. The event when a bi-exciton photon starts the correlation measurement and an exciton photon stops it, positive times in Fig. 4(a), shows a clearly bunched behavior. This is in essence a lifetime measurement of the exciton. The exciton has an increased probability of recombining shortly after the recombination of the bi-exciton. The reason for the long time-scale for positive times in Fig. 4(a) is intriguing. An explanation could be that the exciton is re-excited to the bi-exciton prior to recombining thus prolonging the stop event of the exciton photon to occur. The

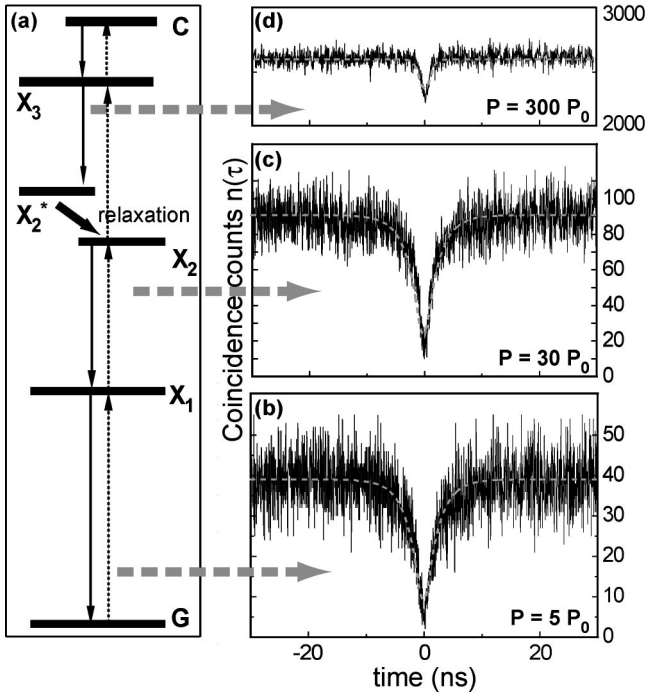

FIG. 3. (a) The decay of the tri-exciton. The tri-exciton X_3 recombines to an excited bi-exciton $X_2^{\star}$ that rapidly relaxes to the bi-exciton ground-state X_2, which in turn recombines through the exciton X_1 to the empty ground-state of the quantum dot G. The solid arrows indicate radiative decay [with corresponding times τ_{X_1}, τ_{X_2}, and τ_{X_3}, in Eq. (1)] whereas the dotted arrows indicate re-excitation of the excitonic levels [with corresponding time τ_E in Eq. (1)]. (b)–(d) Autocorrelation measurements of (b) the exciton, (c) the bi-exciton, and (d) the tri-exciton ($P_0 = 0.1$ W/cm^2). The dashed line is the expected shape for ideal antibunching given our instrumental resolution (800 ps) and a "lifetime" of 2.3, 2.2, and 0.55 ns, for the X_1, X_2, and X_3, respectively.

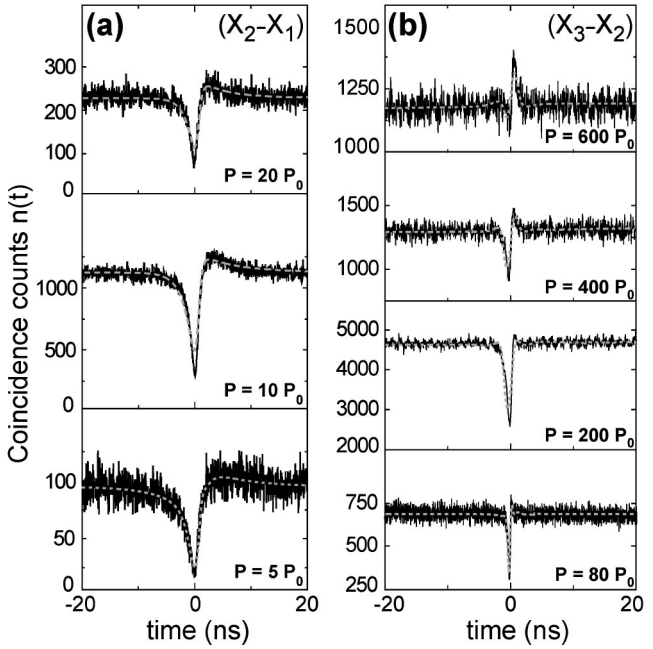

FIG. 4. (a) Cross-correlation of exciton and bi-exciton as a function of excitation power density. From the bottom: $P = 5$ P$_0$, $P = 10$ P$_0$, and $P = 20$ P$_0$ ($P_0 = 0.1$ W/cm^2). Positive times presents the correlation of an exciton photon following a bi-exciton photon, negative times presents the process of a bi-exciton photon following an exciton photon. (b) Cross-correlation of bi-exciton and a tri-exciton as a function of excitation power density. From the bottom: $P = 80$ P$_0$, $P = 200$ P$_0$, $P = 400$ P$_0$, and $P = 600$ P$_0$ ($P_0 = 0.1$ W/cm^2). Positive times presents the correlation of a bi-exciton photon following a tri-exciton photon, negative times presents the process of a tri-exciton photon following a bi-exciton photon.

presence of a dark exciton state would also delay the exciton photon emission, i.e., what we see in Fig. 4(a) is the effective exciton lifetime also containing transitions between a dark and a bright state, predicted to have a long time constant.[24] If we on the other hand start the correlation measurement with the exciton photon and stop it with the bi-exciton photon, negative times in Fig. 4(a), it takes time for the dot to be re-excited, this amounts to a measurement of the recycling time of the quantum dot. This explains the strong antibunching for negative times in the figure. The re-excitation time can be controlled with the excitation intensity. The population rate is directly dependent on the laser power and the re-excitation time therefore decreases when the laser power increases. Due to limited time-resolution of the detection system, the discontinuity at $t = 0$ is washed out resulting in an increase of the correlations at negative times and a reduction in the correlations at positive times.

We have also measured the cross-correlation of the bi-exciton emission with the tri-exciton emission. This is shown in Fig. 4(b). The behavior is similar to the exciton-bi-exciton case, and it is thus clear that there is a three-photon cascaded emission from the tri-exciton via the bi-exciton and the exciton to the quantum dot ground state. Because the experiment was done using a continuous excitation source, it was not possible to correlate the exciton with the tri-exciton, since the exciton is quenched at excitation power densities necessary to obtain a tri-exciton signal, see Fig. 2.

Two additional lines were correlated with the bi-exciton line, emitting at 1.812 and 1.813 eV, visible at high power ($P = 400$ P$_0$) in Fig. 2, but no correlations were obtained. The lines are weak also at high excitation power density and the spectra seem to consist of many competing lines. Also, we cannot dismiss the possibility that some of these emission lines originates from another dot.

In order to support our interpretation of the photon correlation data obtained, we have analyzed the photon cascade using a simple rate equation model.[10,11,25] The rate equations correspond to the schematic shown in Fig. 3(a), where we assumed that only two incoherent processes are responsible for the dynamics of the excitonic states: spontaneous radiative decay and re-excitation with a rate proportional to the excitation power.

$$\frac{dC(t)}{dt} = -\frac{C(t)}{\tau_C} + \frac{X_3(t)}{\tau_E},$$

$$\frac{dX_3(t)}{dt} = -\frac{X_3(t)}{\tau_{X_3}} + \frac{C(t)}{\tau_C} - \frac{X_3(t)}{\tau_E} + \frac{X_2(t)}{\tau_E},$$

$$\frac{dX_2(t)}{dt} = -\frac{X_2(t)}{\tau_{X_2}} + \frac{X_3(t)}{\tau_{X_3}} - \frac{X_2(t)}{\tau_E} + \frac{X_1(t)}{\tau_E},$$

$$\frac{dX_1(t)}{dt} = -\frac{X_1(t)}{\tau_{X_1}} + \frac{X_2(t)}{\tau_{X_2}} - \frac{X_1(t)}{\tau_E} + \frac{G(t)}{\tau_E},$$

$$\frac{dG(t)}{dt} = \frac{X_1(t)}{\tau_{X_1}} - \frac{G(t)}{\tau_E}. \quad (1)$$

X_1, X_2, and X_3 represent the populations of the exciton, bi-exciton, and tri-exciton, respectively, with corresponding decay times τ_{X_1}, τ_{X_2}, and τ_{X_3}. G is the population of the empty ground state and $1/\tau_E$ is the rate of exciting the quantum dot. In order to truncate the ladder of states connected by rates in our model, we have introduced an effective cut-off state C. This accounts for population and depopulation of all higher excited states via excitation and radiative decay, respectively. An analytic solution of these equations is basically a sum of exponentials with different time constants. However, we solved the equations numerically. The fitting parameters have reasonable values and the results, seen as the dashed lines in Fig. 4, give qualitative support of the correlation measurements.

In conclusion, we have demonstrated cascaded photon emission from the decay chain of the tri-exciton, through the bi-exciton and the exciton of a single InP quantum dot. This shows the possibility of creating designed photon triplets with good efficiency at a wavelength suitable for silicon detection. In addition we use the photon correlations to identify the origin of the emission lines in the spectrum of a quantum dot.

We acknowledge W. Seifert for providing the sample and U. Håkanson for assistance in the sample processing. R. Zimmermann and M.-E. Pistol are acknowledged for helpful discussions. This work was supported by the Deutsche Forschungsgemeinschaft (DFG, Grant No. 2224/1), the Swedish Research Council (VR), and the Swedish Foundation for Strategic Research (SSF). V.Z. acknowledges funding from the European Union.

*Electronic address: jonas.persson@ftf.lth.se
†Now at: Institute of Quantum Electronics, ETH Hönggerberg, CH-8093 Zürich, Switzerland.

[1] A. Kuhn, M. Hennrich, and G. Rempe, Phys. Rev. Lett. **89**, 067901 (2002).
[2] B. Lounis and W. E. Moerner, Nature (London) **407**, 491 (2000).
[3] C. Brunel, B. Lounis, P. Tamarat, and M. Orrit, Phys. Rev. Lett. **83**, 2722 (1999).
[4] C. Kurtsiefer, S. Mayer, P. Zarda, and H. Weinfurter, Phys. Rev. Lett. **85**, 290 (2000).
[5] R. Brouri, A. Beveratos, J.-P. Poizat, and P. Grangier, Opt. Lett. **25**, 1294 (2000).
[6] P. Michler, A. Imamoglu, M. D. Mason, P. J. Carson, G. F. Strouse, and S. K. Buratto, Nature (London) **406**, 268 (2000).
[7] P. Michler, A. Kiraz, C. Becher, W. V. Shoenfeld, P. M. Petroff, L. Zhang, E. Hu, and A. Imamoglu, Science **290**, 2282 (2000).
[8] C. Santori, M. Pelton, G. Solomon, Y. Dale, and Y. Yamamoto, Phys. Rev. Lett. **86**, 1502 (2001).
[9] V. Zwiller, H. Blom, P. Jonsson, N. Panev, S. Jeppesen, T. Tsegaye, E. Goobar, M.-E. Pistol, L. Samuelson, and G. Björk, Appl. Phys. Lett. **78**, 2476 (2001).
[10] D. V. Regelman, U. Mizrahi, D. Gershoni, E. Ehrenfreund, W. V. Schoenfeld, and P. M. Petroff, Phys. Rev. Lett. **87**, 257401 (2001).
[11] E. Moreau, I. Robert, L. Manin, V. Thierry-Mieg, J. M. Gérard, and I. Abram, Phys. Rev. Lett. **87**, 183601 (2001).
[12] A. Kiraz, S. Fälth, C. Becher, B. Gayral, W. V. Schoenfeld, P. M. Petroff, L. Zhang, E. Hu, and A. Imamoglu, Phys. Rev. B **65**, 161303 (2002).
[13] O. Benson, C. Santori, M. Pelton, and Y. Yamamoto, Phys. Rev. Lett. **84**, 2513 (2000).
[14] C. Santori, D. F. M. Pelton, G. Solomon, and Y. Yamamoto, Phys. Rev. B **66**, 045308 (2002).
[15] A. J. Berglund, A. C. Doherty, and H. Mabuchi, Phys. Rev. Lett. **89**, 068101 (2002).
[16] K. Sebald, P. Michler, T. Passow, D. Hommel, G. Bacher, and A. Forchel, Appl. Phys. Lett. **81**, 2920 (2002).
[17] T. Aichele, V. Zwiller, O. Benson, I. Akimov, and F. Henneberger, J. Opt. Soc. Am. A **20**, 2189 (2003).
[18] V. Zwiller, T. Aichele, W. Seifert, J. Persson, and O. Benson, Appl. Phys. Lett. **82**, 1509 (2003).
[19] J. Persson, M. Holm, C. Pryor, D. Hessman, W. Seifert, L. Samuelson, and M.-E. Pistol, Phys. Rev. B **67**, 035320 (2003).
[20] N. Carlsson, W. Seifert, A. Peterson, P. Castrillo, M.-E. Pistol, and L. Samuelson, Appl. Phys. Lett. **65**, 3093 (1994).
[21] D. Hessman, J. Persson, M.-E. Pistol, C. Pryor, and L. Samuelson, Phys. Rev. B **64**, 233308 (2001).
[22] U. Håkanson, J. Persson, F. Persson, H. Svensson, L. Montelius, and M. K.-J. Johansson, Nanotechnology **14**, 675 (2003).
[23] R. H. Brown and R. Q. Twiss, Nature (London) **178**, 1447 (1956).
[24] L. Landin, M.-E. Pistol, C. Pryor, M. Persson, L. Samuelson, and M. Miller, Phys. Rev. B **60**, 16 640 (1999).
[25] V. Zwiller, M. E. Pistol, D. Hessman, R. Cederström, W. Seifert, and L. Samuelson, Phys. Rev. B **59**, 5021 (1999).